THE JOURNAL OF BIOLOGICAL CHEMISTRY Vol. 277, No. 16, Issue of April 19, pp. 14238–14245, 2002
Printed in U.S.A.

Design of a Novel Peptide Inhibitor of HIV Fusion That Disrupts the Internal Trimeric Coiled-coil of gp41*

Received for publication, February 12, 2002
Published, JBC Papers in Press, February 21, 2002, DOI 10.1074/jbc.M201453200

Carole A. Bewley‡, John M. Louis, Rodolfo Ghirlando, and G. Marius Clore§

From the Laboratories of Bioorganic Chemistry, Chemical Physics, and Molecular Biology, NIDDK, National Institutes of Health, Bethesda, Maryland 20892

The pre-hairpin intermediate of gp41 from the human immunodeficiency virus (HIV) is the target for two classes of fusion inhibitors that bind to the C-terminal region or the trimeric coiled-coil of N-terminal helices, thereby preventing formation of the fusogenic trimer of hairpins. Using rational design, two 36-residue peptides, $N36^{Mut(e,g)}$ and $N36^{Mut(a,d)}$, were derived from the parent N36 peptide comprising the N-terminal helix of the gp41 ectodomain (residues 546–581 of HIV-1 envelope), characterized by analytical ultracentrifugation and CD, and assessed for their ability to inhibit HIV fusion using a quantitative vaccinia virus-based fusion assay. $N36^{Mut(e,g)}$ contains nine amino acid substitutions designed to disrupt interactions with the C-terminal region of gp41 while preserving contacts governing the formation of the trimeric coiled-coil. $N36^{Mut(a,d)}$ contains nine substitutions designed to block formation of the trimeric coiled-coil but retains residues that interact with the C-terminal region of gp41. $N36^{Mut(a,d)}$ is monomeric, is largely random coil, does not interact with the C34 peptide derived from the C-terminal region of gp41 (residues 628–661), and does not inhibit fusion. The trimeric coiled-coil structure is therefore a prerequisite for interaction with the C-terminal region of gp41. $N36^{Mut(e,g)}$ forms a monodisperse, helical trimer in solution, does not interact with C34, and yet inhibits fusion about 50-fold more effectively than the parent N36 peptide (IC_{50} ~ 308 nM *versus* ~16 μM). These results indicate that $N36^{Mut(e,g)}$ acts by disrupting the homotrimeric coiled-coil of N-terminal helices in the pre-hairpin intermediate to form heterotrimers. Thus $N36^{Mut(e,g)}$ represents a novel third class of gp41-targeted HIV fusion inhibitor. A quantitative model describing the interaction of $N36^{Mut(e,g)}$ with the pre-hairpin intermediate is presented.

Virus-cell and cell-cell fusion mediated by the viral envelope glycoproteins (Env)[1] (1) gp41 and gp120 constitute the first step of infection and dissemination, respectively, of the human immunodeficiency virus (HIV) and hence represent a promising target for the development of antiviral therapeutics (2). Following binding of gp120 to CD4 and a chemokine receptor, a conformational change occurs in the gp120/gp41 oligomer that leads to insertion of the fusion peptide of gp41 into the target membrane and ultimately membrane fusion (2, 3). The structure of the ectodomain of both HIV and simian immunodeficiency virus gp41 in its fusogenic/postfusogenic state has been solved by NMR (4) and crystallography (5–8) and shown to consist of a trimer of hairpins. Each subunit comprises long N- and C-terminal helices connected by a 25–30-residue loop. The N-helices form a parallel, trimeric coiled-coil in the interior of the complex surrounded by the C-terminal helices oriented antiparallel to the N-terminal helices (Fig. 1*a*, *bottom*). Peptides derived from the C- and N-helices inhibit Env-mediated fusion at nanomolar and micromolar concentrations, respectively (9–12). These peptides do not bind the fusion-active or postfusogenic state of gp41 as represented by the ectodomain of gp41 free in solution and are thought to interact with a pre-hairpin intermediate (2, 13, 14) in which the N- and C-helices are not associated and the trimeric coiled-coil of N-helices is exposed (Fig. 1*a*, *top left*). Peptides derived from the C-terminal helix, such as C34 (residues 628–661 of HIV-1 Env) and T20 (residues 638–673 of HIV-1 Env; currently in phase III clinical trials (15, 16)) target the exposed face of the trimeric coiled-coil of N-helices (11, 13, 14, 17, 18). Engineered constructs such as the chimeric protein N_{CCG}-gp41 (19), which features an exposed, stable, disulfide-linked, trimeric coiled-coil of N-helices grafted onto the minimal, thermostable ectodomain of gp41; peptides in which the trimeric coiled-coil of N-helices is stabilized by fusion to the GCN4 trimeric coiled-coil (12); and the protein 5-helix (20), in which the internal trimeric coiled-coil of N-helices is surrounded by only two C-helices, specifically target the C-region in the pre-hairpin intermediate state (Fig. 1*a*, *top left*). In both instances, packing of the C-region onto the trimeric coiled-coil of N-helices is blocked, and hairpin formation is inhibited. Although the ectodomain of gp41 in free solution is highly thermostable (with a T_m in excess of 100 °C) (21), it has been shown to exist as a monomer-trimer equilibrium (21, 22). In the context of the fusion process, the trimeric coiled-coil of N-helices in the pre-hairpin intermediate state may also exist as a monomer-trimer equilibrium (4, 22, 23). If this is indeed the case, blocking the formation of the fusion-competent, homotrimeric coiled-coil of N-helices may provide another molecular target for

* This work was supported by the Intramural AIDS Targeted Antiviral Program of the Office of the Director of the National Institutes of Health (to G. M. C. and C. A. B.). The costs of publication of this article were defrayed in part by the payment of page charges. This article must therefore be hereby marked "*advertisement*" in accordance with 18 U.S.C. Section 1734 solely to indicate this fact.

‡ To whom correspondence may be addressed: Laboratory of Bioorganic Chemistry, Bldg. 8, NIDDK, National Institutes of Health, Bethesda, MD 20892-0820. Tel.: 301-594-5187; E-mail: caroleb@intra.niddk.nih.gov.

§ To whom correspondence may be addressed: Laboratory of Chemical Physics, Bldg. 5, Rm. B1-30I, NIDDK, National Institutes of Health, Bethesda, MD 20892-0510. Tel.: 301-496-0782; Fax: 301-496-0825; E-mail: clore@speck.niddk.nih.gov.

[1] The abbreviations used are: Env, viral envelope glycoprotein(s); HIV, human immunodeficiency virus; gp120, surface envelope glycoprotein of HIV; gp41, transmembrane subunit of HIV envelope; N36 and C34, peptides encompassing residues 546–581 and 628–661 of HIV-1 Env, respectively; $N36^{Mut(e,g)}$, peptide derived from N36 that contains nine substitutions at positions *e* and *g* of the helical wheel (defined in the context of the gp41 trimer of hairpins structure) corresponding to residues 549, 551, 556, 558, 563, 565, 570, 572, and 577 of HIV-1 Env; $N36^{Mut(a,d)}$, peptide derived from N36 that contains nine substitutions at positions *a* and *d* of the helical wheel (defined in the context of the gp41 trimer of hairpins structure) corresponding to residues 552, 555, 559, 562, 566, 569, 573, 576, and 580 of HIV-1 Env.

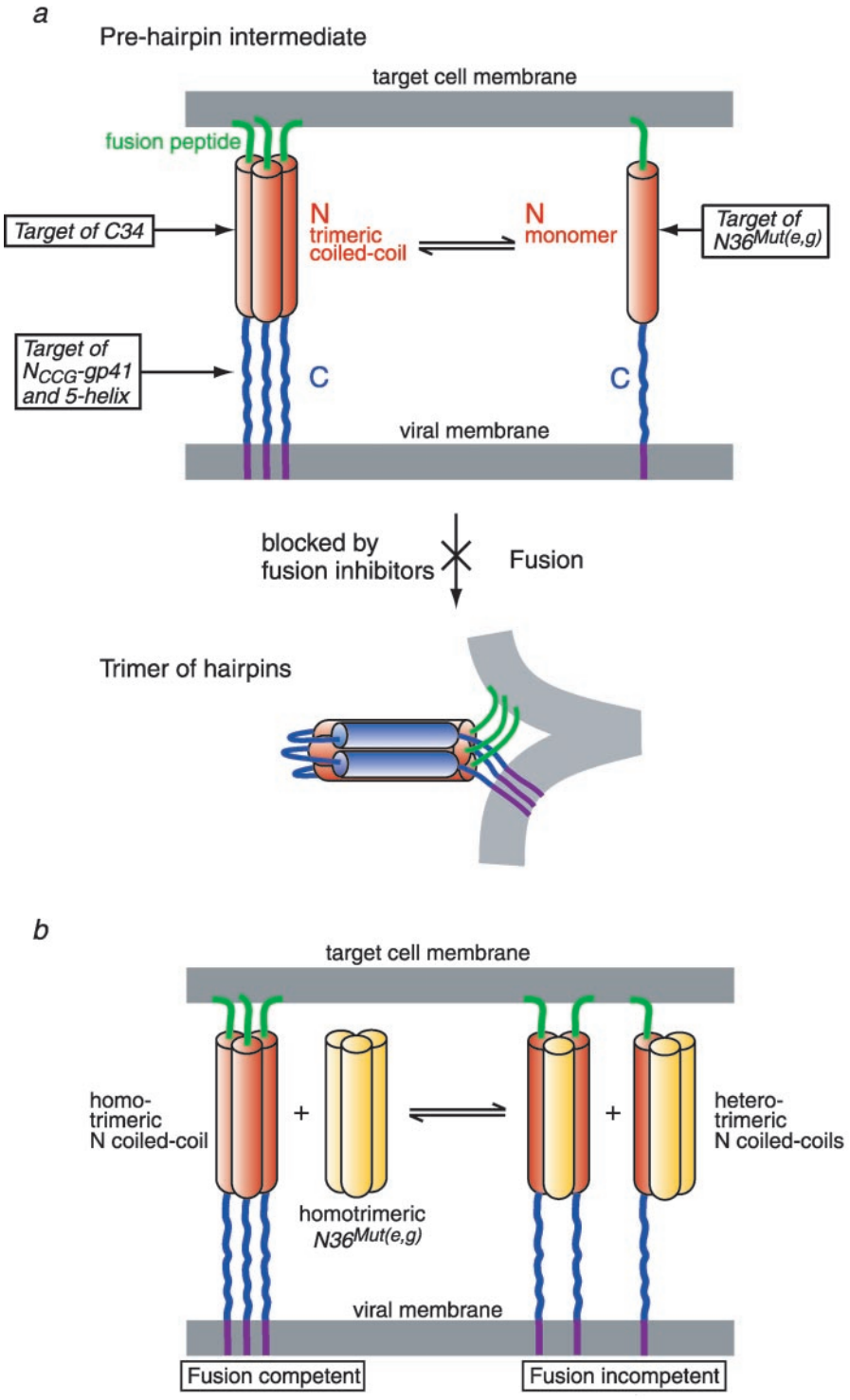

FIG. 1. **Schematic model illustrating the site of action of different HIV fusion inhibitors that target the ectodomain of gp41.** *a*, the fusogenic state of gp41 (*bottom*) consists of a trimer of hairpins comprising an internal trimeric, helical coiled-coil of the N-region (*red*) surrounded by helices derived from the C-region (*blue*) (4–8). The inhibitors target a pre-hairpin intermediate state (*top*) in which the N- (*red*) and C- (*blue*) regions of gp41 are not yet associated (2). In the pre-hairpin intermediate state, the N-region (*red*) is thought to consist of a trimeric, parallel helical coiled-coil; the fusion peptide (*green*) located at the N terminus of the ectodomain of gp41 is inserted into the target cell membrane; the C-region (*blue*) of gp41 is anchored to the viral membrane by a transmembrane segment (*purple*). Peptides derived from the C-region, such as C34 (11), bind to the N-region in its trimeric coiled-coil state; the proteins N_{CCG}-gp41 (19) and 5-helix (20), which expose either the complete or a portion of the N-region trimeric coil-coil in a stable form, bind to the C-region. $N36^{Mut(e,g)}$, the subject of the present article, has been designed to remove the interaction surface between the N- and C-regions and therefore can only interact with the N-region in a monomeric form, thereby disrupting the homotrimeric coiled-coil N-region and resulting in the formation of heterotrimers. In all three instances, the fusion inhibitors block the formation of the trimer of hairpins, thereby preventing apposition of the viral and target cell membranes. *b*, as a consequence of the existence of a monomer-trimer equilibrium for the trimeric coiled-coil of N-helices, the interaction of homotrimeric $N36^{Mut(e,g)}$ (*yellow*) with the fusion-competent homotrimeric pre-hairpin intermediate (N-helices in *red*) results in subunit exchange and the formation of fusion-incompetent heterotrimers.

inhibiting HIV cell fusion. In this article, we present the design and characterization of a peptide, derived from the N-helix of gp41, in which the sites of interaction with the C-helices have been mutated, but the sites of intermolecular contacts between the N-helices have been preserved. This peptide, which we term $N36^{Mut(e,g)}$, is about 50-fold more effective in inhibiting HIV Env-mediated cell fusion than the N36 peptide (residues 546–581 of HIV-1 Env) of gp41 from which it was derived. These data strongly suggest that the homotrimeric coiled-coil of N-helices in the pre-hairpin state can be disrupted.

EXPERIMENTAL PROCEDURES

Peptides—All peptides (Fig. 2*b*), purchased from Commonwealth Biotechnologies (Richmond, VA), were synthesized on a solid phase support, purified by reverse phase high pressure liquid chromatography, and verified for purity by mass spectrometry and amino acid composition. All peptides bear an acetyl group at the N terminus and an amide group at the C terminus. Concentrations of peptides were determined spectrophotometrically: the calculated A_{280} values (1-cm path length) for a concentration of 1 mg/ml N36, $N36^{Mut(e,g)}$, $N36^{Mut(a,d)}$, and C34 are 1.35, 1.31, 1.34, and 2.90, respectively. The corresponding molecular masses are 4160, 4293, 4182, and 4286 Da, respectively.

Circular Dichroism—CD spectra of peptides (at a concentration cor-

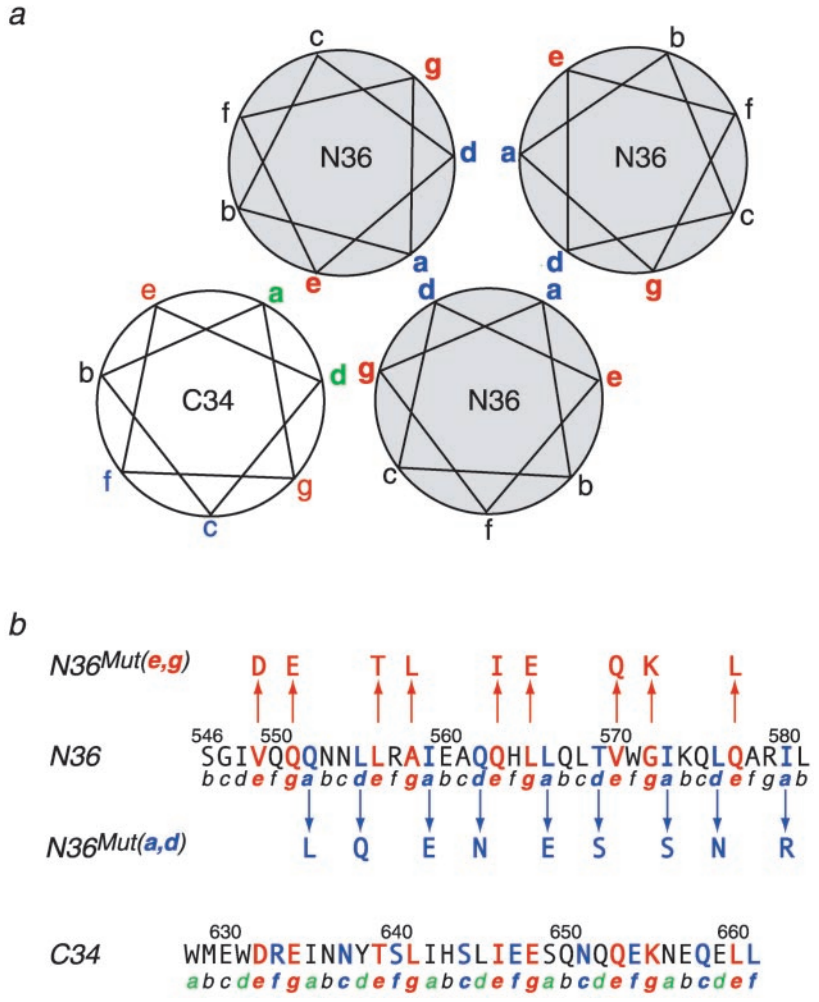

FIG. 2. **Design of a peptide that disrupts the internal N-region trimeric coiled-coil in the pre-hairpin intermediate state of gp41.** *a*, helical wheel representation illustrating the interaction between the N- and C-regions of gp41 in the trimer of hairpins as observed in the solution (4) and crystal (5–8) structures of the fusogenic/postfusogenic state of the ectodomain of gp41. The intermolecular contacts between the N-helices occur between *positions a* and *d* of the helical wheel. Contacts between the N- and C-helices (intra- and intermolecular) involves residues at *positions e* and *g* of the N-helices and *positions a* and *d* of the C-helices. *b*, peptide sequences. The N36 peptide comprises residues 546–581 of the N-region of HIV-1 gp41, and the C34 peptide comprises residues 628–661 of the C-region of HIV-1 gp41. N36 and C34 associate to form a six-helix bundle whose structure has been solved crystallographically (5). In the $N36^{Mut(e,g)}$ mutant, the residues at *positions e* and *g* of N36 have been substituted by residues at *positions e* and *g*, respectively, of C34; this effectively removes the interaction surface with C34 but preserves the contacts necessary to form a trimeric coiled-coil of N-helices. In the $N36^{Mut(a,d)}$ mutant, the residues at *positions a* and *d* of N36 have been substituted by residues at *positions f* and *c*, respectively, of C34; this removes the contacts necessary to form the trimeric coil-coil of N-helices but preserves the interaction sites with C34.

responding to 0.7–0.8 A_{280}) were recorded at 25 °C on a JASCO J-720 spectropolarimeter using a 0.05-cm path length cell. Quantitative evaluation of secondary structure from the CD spectrum was carried out using the program CDNN (www.bioinformatik.biochemtech.uni-halle.de/cd_spect/index.html; Ref. 24).

Sedimentation Equilibrium—Sedimentation equilibrium experiments were conducted at 20.0 °C and three different rotor speeds (16,000, 20,000, and 24,000) on a Beckman Optima XL-A analytical ultracentrifuge. Peptide samples were prepared in 50 mM sodium formate buffer (pH = 3) and loaded into the ultracentrifuge cells at nominal loading concentrations of ~0.2 and 0.7–0.8 A_{280}. Data were analyzed in terms of a single ideal solute to obtain the buoyant molecular mass, $M(1 - v\rho)$, using the Optima XL-A data analysis software (Beckman). The value for the experimental molecular mass M was determined using calculated values for the density ρ (determined at 20 °C using standard tables) and partial specific volume v (calculated on the basis of amino acid composition (25)).

Cell Fusion Assay—Inhibition of HIV Env-mediated cell fusion by peptides was carried out as described previously (19) using a modification (26) of the vaccinia virus-based reporter gene assay (using soluble CD4 at a final concentration of 200 nM). B-SC-1 cells were used for both target and effector cell populations. Target cells were co-infected with vCB21R-LacZ and vCBYF1-fusin (CXCR4), and effector cells were co-infected with vCB41 (Env) and vP11T7gene1 at a multiplicity of infection of 10. For inhibition studies, peptides were added to an appropriate volume of Dulbecco's modified Eagle's medium (2.5%) and phosphate-buffered saline to yield identical buffer compositions (100 μl) followed by addition of 1×10^5 effector cells (in 50 μl of medium) per well. After incubation for 15 min, 1×10^5 target cells (in 50 μl) and soluble CD4 were added to each well. Following 2.5 h of incubation, β-galactosidase activity of cell lysates was measured (A_{570}; Molecular Devices 96-well spectrophotometer) upon addition of chlorophenol red-β-D-galactopyranoside (Roche Molecular Biochemicals). The curves for %fusion *versus* peptide inhibitor concentration were fit by nonlinear least-squares optimization using the program FACSIMILE (27, 28).

RESULTS AND DISCUSSION

Design of Peptide Inhibitors—The helical wheel diagram in Fig. 2*a* illustrates the interactions between the N-helices and between the N- and C-helices as observed in both the NMR (4) and x-ray (5–8) structures of the fusogenic/postfusogenic state of the ectodomain of gp41. Internal contacts between the N-helices involve positions *a* and *d* of the helical wheel (5). Each C-helix interacts with two N-helices (one intra- and the other intersubunit): these contacts involve positions *e* and *g* of the N-helices and positions *a* and *d* of the C-helix (5). The first crystal structure of the HIV-1 gp41 ectodomain core consisted of a complex of N36 and C34 peptides comprising residues 546–581 and 628–661, respectively, of HIV-1 Env (5). Using the N36 and C34 peptides as starting points, we designed two peptides: $N36^{Mut(e,g)}$, which can only undergo self-association but cannot interact with C34, and $N36^{Mut(a,d)}$, which can no longer self-associate but could potentially still interact with C34 (Fig. 2*b*). In the case of $N36^{Mut(e,g)}$, the residues at positions *e* and *g* of N36 have been replaced by residues at positions *e* and *g* of C34. Since the latter residues are located on the external surface of C34 in the context of the ectodomain gp41 core (4–8) and since C34 on its own is monomeric (29),[2] this set

[2] C. A. Bewley, J. M. Louis, R. Ghirlando, and G. M. Clore, unpublished data.

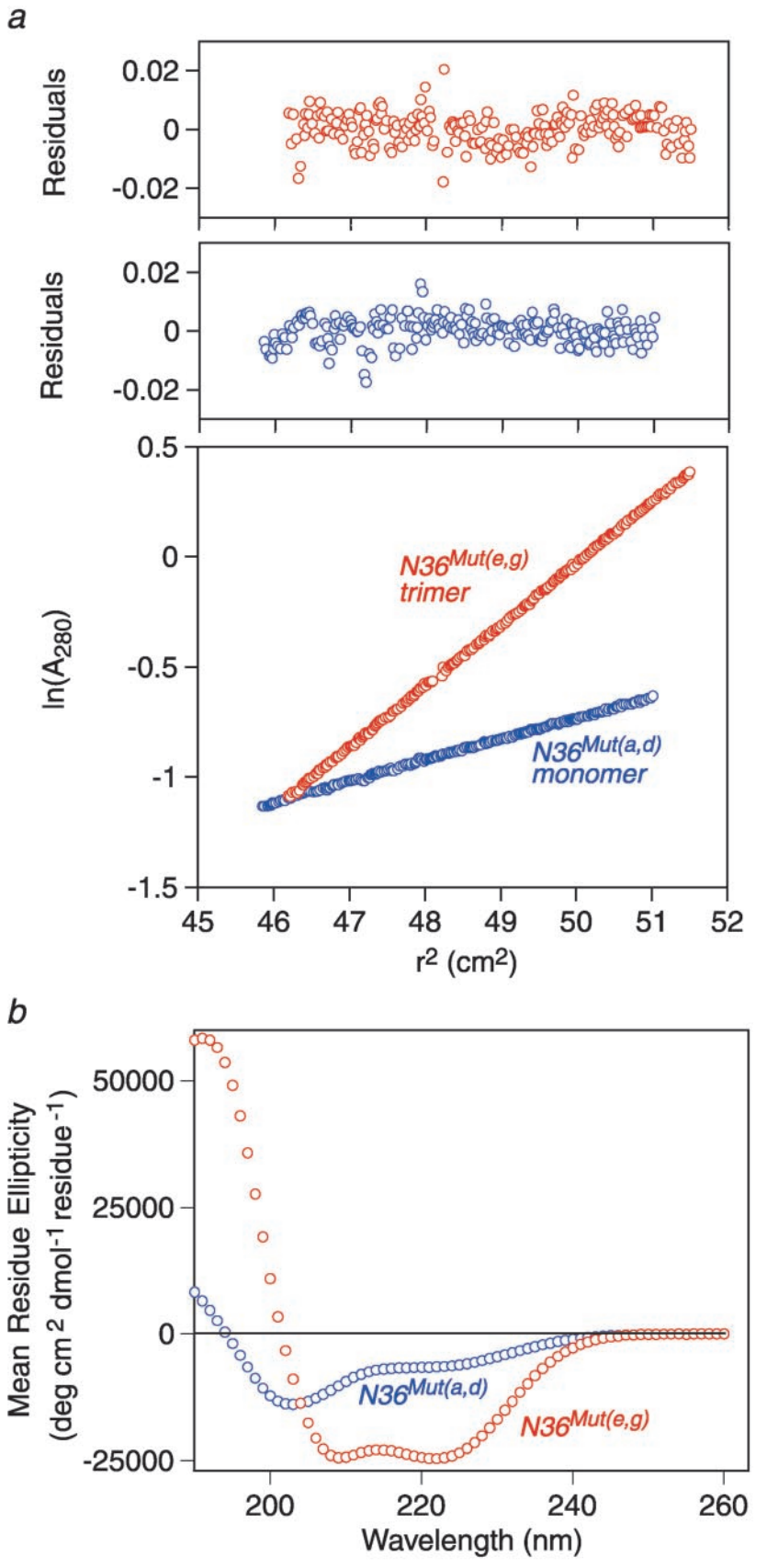

FIG. 3. **Characterization of $N36^{Mut(e,g)}$ (*red*) and $N36^{Mut(a,d)}$ (*blue*).** *a*, results of analytical ultracentrifugation on $N36^{Mut(e,g)}$ and $N36^{Mut(a,d)}$. Sedimentation equilibrium profiles, plotted in terms of $\ln(A_{280})$ *versus* the square of the radius (r^2) (*bottom panel*), are shown; also shown in the *top two panels* is the distribution of residuals between calculated and experimental data for best fits to a monomer of $N36^{Mut(a,d)}$ and a trimer of $N36^{Mut(e,g)}$. The concentrations (in monomer) of $N36^{Mut(a,d)}$ and $N36^{Mut(e,g)}$ are ~140 μM (A_{280} ~ 0.8) and 124 μM (A_{280} ~ 0.7), respectively. The calculated molecular masses are 3660 ± 80 Da for $N36^{Mut(a,d)}$, which corresponds to a monomer, and 12,040 ± 200 Da for $N36^{Mut(e,g)}$, which corresponds to a trimer. An independent run for $N36^{Mut(e,g)}$ at a concentration of 36 μM in monomer (A_{280} ~ 0.2) yielded a molecular mass of 12,500 ± 180 Da. *b*, CD spectrum of $N36^{Mut(e,g)}$ and $N36^{Mut(a,d)}$. The calculated helical content is ~80% for $N36^{Mut(e,g)}$ and ~20% for $N36^{Mut(a,d)}$. *deg*, degrees.

of substitutions will prevent any interaction between $N36^{Mut(e,g)}$ and the C-region of gp41 in its pre-hairpin intermediate state while preserving the intermolecular contacts required to form the trimeric coiled-coil of N-helices. In the case of $N36^{Mut(a,d)}$, the residues at positions *a* and *d* of N36 have been substituted by residues at positions *f* and *c* of C34, which

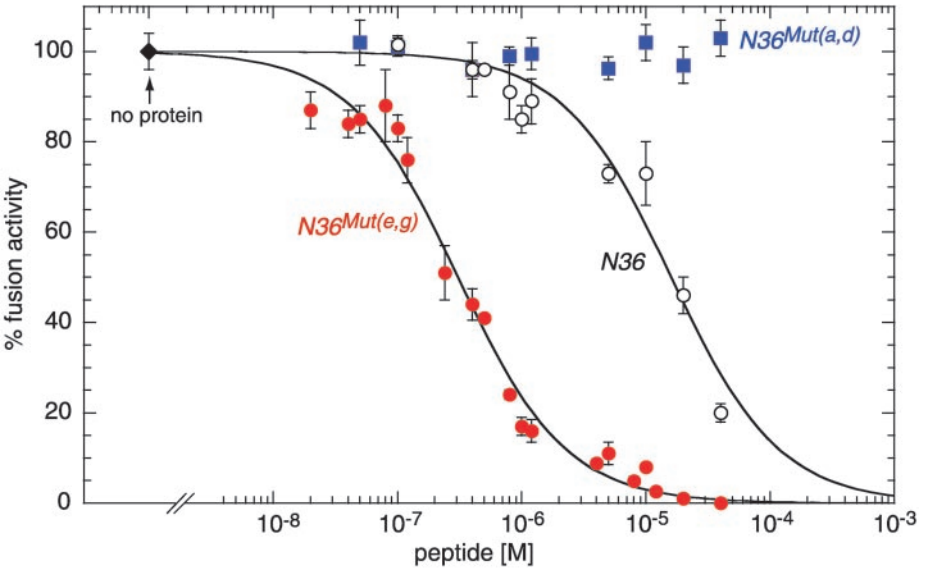

FIG. 4. **Inhibition of HIV Env-mediated cell fusion by $N36^{Mut(e,g)}$, $N36^{Mut(a,d)}$, and N36.** *Red solid circles*, $N36^{Mut(e,g)}$; *blue solid squares*, $N36^{Mut(a,d)}$; *black open circles*, N36.The *solid lines* represent best fits to the data using the simple activity relationship: %fusion = $100/(1+[I]/IC_{50})$ where [I] is the inhibitor concentration. The IC_{50} values for $N36^{Mut(e,g)}$ and N36 are 308 ± 22 nM and 16 ± 2 μM, respectively. $N36^{Mut(a,d)}$ displays no inhibitory activity at the concentrations tested.

are located on the solvent-exposed face of the ectodomain core of gp41 (4–8), thereby removing the intermolecular contacts required to form the trimeric coiled-coil of N-helices.

Biophysical Characterization of $N36^{Mut(e,g)}$ and $N36^{Mut(a,d)}$—The results of analytical ultracentrifugation on $N36^{Mut(e,g)}$ and $N36^{Mut(a,d)}$ are presented in Fig. 3*a*. $N36^{Mut(e,g)}$ behaves as a single monodisperse species at concentrations of ~36 μM (in monomer; A_{280} ~ 0.2) and ~124 μM (in monomer; A_{280} ~ 0.7) with a molecular mass of ~12,000–12,500 Da, corresponding to a trimer. In this context it is worth noting that N36 on its own aggregates and does not form a well defined trimer (12),[2] presumably due to further self-association involving the predominantly hydrophobic residues at positions *e* and *g*, which have been substituted by predominantly hydrophilic residues in $N36^{Mut(e,g)}$ (Fig. 2*b*). $N36^{Mut(a,d)}$ also behaves as a single monodisperse species at a concentration of ~140 μM (A_{280} ~ 0.8), but its molecular mass is only ~3700 Da, corresponding to a monomer.

CD spectra of $N36^{Mut(e,g)}$ and $N36^{Mut(a,d)}$ are shown in Fig. 3*b*. $N36^{Mut(e,g)}$ displays a double minimum at 208 and 222 nm, characteristic of an α-helix; and quantification of the CD data (24) indicates a helical content of ~80%. $N36^{Mut(a,d)}$, on the other hand, is largely random coil (characterized by a minimum around 200 nm) with a small amount of α-helix (~20%).

We were unable to detect any evidence of interaction between either $N36^{Mut(e,g)}$ or $N36^{Mut(a,d)}$ and C34 by either analytical ultracentrifugation or CD. The absence of interaction between $N36^{Mut(e,g)}$ and C34 is exactly as predicted from the design since the points of contact with C34 have been mutated (*cf.* Fig. 2). The absence of interaction between $N36^{Mut(a,d)}$ and C34 was initially somewhat surprising since the residues that contact C34 in the context of the fusogenic/postfusogenic state of the gp41 ectodomain were preserved. This result therefore indicates that C34 can only form a complex with a stable trimeric coiled-coil of N-helices. From a structural standpoint, this is readily understood since each C-helix contacts two N-helices of the trimeric coiled-coil (one intramolecular and the other intersubunit; *cf.* Fig. 2*a*), and the buried surface area for each of the two interactions is comparable.

To exclude the remote possibility that $N36^{Mut(e,g)}$ could behave in a manner analogous to C34 and bind to the surface of the trimeric coiled-coil of N-helices in the pre-hairpin intermediate of gp41, we also examined the interaction of $N36^{Mut(e,g)}$ with the engineered protein N_{CCG}-gp41. N_{CCG}-gp41 is a chimeric protein that features an exposed trimeric coiled-coil of N-helices that is stabilized both by fusion to a minimal thermostable ectodomain of gp41 and by engineered intersubunit disulfide bonds (19). The exposed trimeric coiled-coil of N-helices in N_{CCG}-gp41 mimics that of the pre-hairpin intermediate of gp41, but in contrast to native gp41, the N-helices cannot dissociate since they are covalently tethered by disulfide bonds. Analytical ultracentrifugation on various mixtures of $N36^{Mut(e,g)}$ and N_{CCG}-gp41 in ratios of 4.5:1 and 11.7:1 (24 μM $N36^{Mut(e,g)}$ plus 5.3 μM N_{CCG}-gp41 and 51 μM $N36^{Mut(e,g)}$ plus 4.4 μM N_{CCG}-gp41, respectively, with concentrations expressed in trimer) provided no evidence of any interactions between these two molecules, and the data were readily accounted for by a mixture of two ideal species.

Inhibition of HIV Env-mediated Cell Fusion—The results of a quantitative vaccinia virus-based reporter gene assay (26) for HIV Env-mediated cell fusion are shown in Fig. 4. N36 inhibits fusion with an IC_{50} of 16 ± 2 μM in agreement with previous results (19). $N36^{Mut(e,g)}$ inhibits fusion with an IC_{50} 308 ± 22 nM. Thus $N36^{Mut(e,g)}$ is ~50-fold more active in inhibiting fusion than N36. $N36^{Mut(a,d)}$, on the other hand, fails to inhibit fusion even at concentrations as high as 0.1 mM. The lack of any fusion-inhibitory activity for $N36^{Mut(a,d)}$ is exactly as predicted from the biophysical data since $N36^{Mut(a,d)}$ does not self-associate and does not interact with C34.

Since $N36^{Mut(e,g)}$ forms a well defined trimeric species that does not interact with either C34 or the chimeric protein N_{CCG}-gp41 (in which the N-helices of the solvent-exposed trimeric coil-coil are covalently linked by interhelical disulfide bonds), it must target the N-region of the pre-hairpin intermediate by forming fusion-incompetent heterotrimers (Fig. 1*b*). Analytical ultracentrifugation on the ectodomain of gp41 indicates the presence of only monomer and trimer species in equilibrium (21, 22); that is, assembly of the trimer is a highly cooperative process. The fusion-inhibitory activity of $N36^{Mut(e,g)}$ therefore indicates the presence of a dynamic equilibrium between monomeric and trimeric forms of membrane-bound gp41 that allows subunit exchange to take place in the pre-hairpin intermediate state. The rate of exchange between these species must be sufficiently fast to permit efficient heterotrimer formation within the lifetime (~15 min) of the pre-hairpin intermediate (13, 30, 31).

Modeling Inhibition of HIV Env-mediated Cell Fusion by $N36^{Mut(e,g)}$—The inhibition curve for $N36^{Mut(e,g)}$ is well fit by a simple Langmuir isotherm given by %fusion = $100/(1 + [N36^{Mut(e,g)}]/IC_{50})$ (Fig. 4). Yet, mechanistically, the interaction

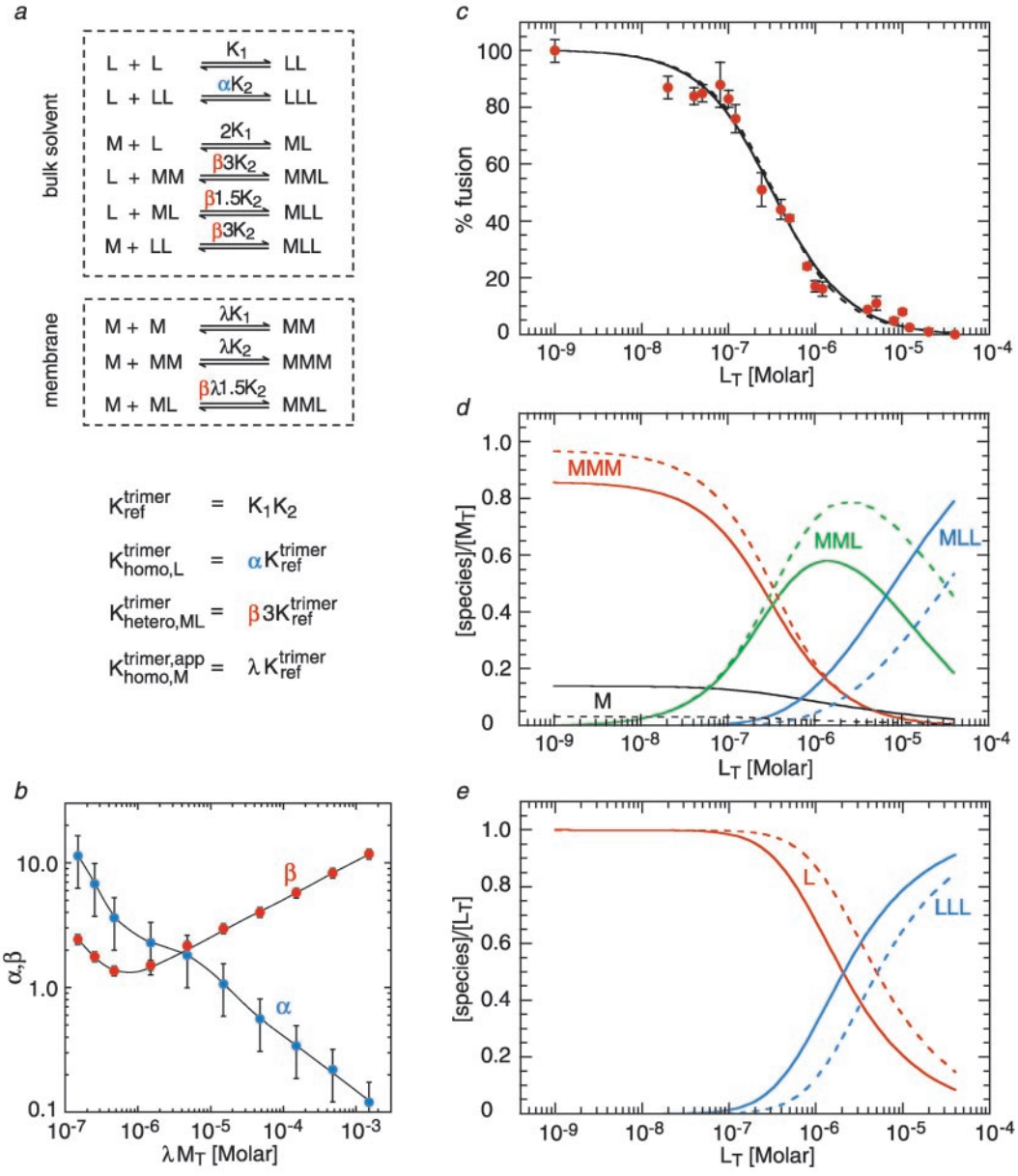

FIG. 5. **Modeling the inhibition of HIV Env-mediated cell fusion by N36$^{Mut(e,g)}$.** *a*, mechanistic scheme. L, LL, and LLL are the monomeric, homodimeric, and homotrimeric forms, respectively, of the ligand N36$^{Mut(eg,)}$; M, MM, and MMM are the monomeric, homodimeric, and homotrimeric forms, respectively, of the prefusion intermediate of gp41 bound on the surface of the cell; ML is the heterodimeric species formed by the interaction of M and L; MML and MLL are the heterotrimeric species. K_{ref}^{trimer} is the experimentally measured equilibrium association constant for the monomer-trimer equilibrium of the ectodomain of gp41 in free solution (4.8×10^{11} M^{-2}; Ref. 21) given by the product of K_1 and K_2 with $K_2 \gg K_1$ (since trimer formation is highly cooperative, and only monomer and trimer species can be detected by analytical ultracentrifugation). (K_1 was arbitrarily set to 10^4 M^{-1}, yielding a value of 4.8×10^7 M^{-1} for K_2.) The factors α, β, and λ relate the equilibrium association constants for homotrimerization of L ($K_{homo,L}^{trimer}$), heterotrimerization of M and L ($K_{hetero,ML}^{trimer}$), and homodimerization of M ($K_{homo,M}^{trimer,app}$) to K_{ref}^{trimer}. The factor λ serves to convert the concentrations of species in the membrane to their bulk solution concentrations and, in addition, subsumes any energetic differences between trimerization of the pre-hairpin intermediate of gp41 in the membrane and trimerization of the ectodomain of gp41 measured in free solution. The various numerical factors in front of the equilibrium constants are statistical factors related to symmetry considerations involved in the formation of homo- and hetero-oligomeric species. *b*, variation in the optimized values of α and β derived by nonlinear least-squares optimization as a function of λM_T, where M_T is the total concentration of protein (monomer units) in bulk solution. The *vertical bars* represent the error in the fitted parameters. *c*, comparison of the experimental fusion data (*solid red circles*) with the best fit theoretical curves calculated for $\lambda M_T = 1.5 \times 10^{-5}$ M (*solid line*) and 1.5×10^{-4} M (*dashed line*). (For a value of 10 pM for M_T, the corresponding values of λ are 1.5×10^6–1.5×10^7, respectively). The percentage of fusion activity is given by $100[MMM]_{L_T}/[MMM]_{L_{T=0}}$. Note that the two theoretical curves are essentially indistinguishable not only from each other but also from a simple Langmuir isotherm. Calculated fractional concentrations of various species as a function of total protein concentration, M_T (*d*), and total ligand concentration, L_T (*e*). The fraction of dimeric species (*i.e.* $2[MM]/M_T$, $[ML]/M_T$, and $2[LL]/L_T$) is less than 1% for all values of L_T. The curves obtained for $\lambda M_T = 1.5 \times 10^{-5}$ M and 1.5×10^{-4} M are shown as *solid* and *dashed lines*, respectively.

of N36$^{Mut(e,g)}$ with the pre-hairpin intermediate of gp41 is far more complex, involving multiple species in different homo- and hetero-oligomerization states. The simplest scheme describing the situation is presented in Fig. 5*a*. L and M represent N36$^{Mut(e,g)}$ and the pre-hairpin intermediate of gp41 in their monomeric forms, respectively; LL and MM are homodimers; ML is a heterodimer; LLL and MMM are homotrimers; and MML and MLL are heterodimers. We assume that only the homotrimer MMM is fusion-active, and the fraction fusion activity is given by the ratio of $[MMM]_{L_T}/[MMM]_{L_{T=0}}$.

The interactions between ligand (in its various oligomerization states) and membrane-bound protein (in its various homo- and hetero-oligomeric states) are described by their respective bulk solution concentrations. The interactions involving only membrane-bound species, however, are dependent on their concentrations in the two-dimensional membrane (*i.e.* number of molecules per unit area) that are much higher than their concentrations in bulk solvent. In terms of thermodynamics, all equilibria in Fig. 5*a* can be related to the species concentrations in bulk solvent by multiplying the relevant equilibrium constants by a factor λ to yield appropriate apparent equilibrium constants (Fig. 5*a*, *middle panel*).

The measured equilibrium association constant K_{ref}^{trimer} for the ectodomain of HIV-1 gp41 in free solution (*i.e.* the trimer of hairpins) is 4.8×10^{11} M^{-2} and is given by the product of the equilibrium association constants K_1 (monomer-dimer equilibrium) and K_2 (dimer-trimer equilibrium) (Fig. 5*a*, *bottom panel*). Since trimerization of the gp41 ectodomain is highly cooperative (21, 22), $K_2 \gg K_1$. Taking K_{ref}^{trimer} as a reference point, the overall equilibrium association constant between monomeric and homotrimeric species of L is given by αK_{ref}^{trimer}, between monomeric and homotrimeric species of M by λK_{ref}^{trimer} (note that λ also subsumes any difference in the energetics of trimerization between the pre-hairpin intermediate in the membrane and the ectodomain of gp41 in free solution), and between monomeric species of L and M and heterotrimeric species of M and L by $3\beta K_{ref}^{trimer}$ (where the factor 3 is a statistical factor). The scheme in Fig. 5*a* has three unknowns: α, β, and λM_T, where M_T is the total protein concentration (in monomer units). The data, however, are insufficient to determine all three parameters independently. Nonlinear least-squares fitting to the experimental data, optimizing the values of α and β, was carried out for values of λM_T ranging from 1.5×10^{-7} to 1.5×10^{-3} M (which corresponds to values of λ of 1.5×10^4–1.5×10^8 for $M_T = 10$ pM, the probable concentration of protein in bulk solution, estimated on the basis of a concentration of 5×10^3 cells/μl and ~5000 gp41 trimers/cell). (Note that the concentrations of the various species in the scheme shown in Fig. 5*a* as a function of total ligand concentration, L_T, were calculated numerically by integration of the differential equations describing the reactions to essentially infinite time.) The optimized values of α and β depend on the product λM_T, and the results are therefore equally valid for a wide range of M_T concentrations. The data can be equally well fitted for values of λM_T ranging from 10^{-7} to 10^{-3} M with α varying from ~10 to 0.1 and β varying from 1 to 10 (Fig. 5*b*). Best fits to the experimental fusion inhibition data for $\lambda M_T = 1.5 \times 10^{-5}$ and 1.5×10^{-4} M are shown in Fig. 5*c*; the optimized values of α are 1.07 and 0.34 (with error estimates of ~40%), respectively, and of β are 2.97 and 5.76 (with error estimates of 10%), respectively. The resulting curves are essentially indistinguishable from each other as well as from that obtained with a Langmuir isotherm. The occupancy of the various species relative to M_T and L_T are shown in Fig. 5, *d* and *e*, respectively. For this set of parameters, the fraction M in the trimeric state in the absence of ligand is ~86% for $\lambda M_T = 1.5 \times 10^{-5}$ M and ~97% for $\lambda M_T = 1.5 \times 10^{-4}$ M; the value of L_T at which 50% of L is monomeric is ~2×10^{-6} and 5×10^{-6} M, respectively. The occupancy of homodimeric ligand is less than 1% of L_T; likewise the occupancy of homodimeric (MM) and heterodimeric (LM) protein is less than 1% of M_T for all values of L_T. Both MML and MLL heterotrimers are formed with the MML heterotrimer peaking at concentrations of L_T slightly less than that at which 50% of the ligand is monomeric.

The above calculations reveal two important findings. First, despite the complexities introduced by multiple homo- and hetero-oligomerization states, which might lead one to predict a complex relationship between fusion and total ligand concentration, a scheme such as that depicted in Fig. 5*a* can still yield rather simple inhibition data that is readily characterized by a Langmuir isotherm. Second, the values for the various equilibrium constants for trimerization required to best fit the experimental fusion data are entirely compatible with the experimentally measured value for the equilibrium constant for trimerization of the ectodomain of HIV-1 gp41 in solution.

In the best fit calculations described above and depicted in Fig. 5, only the homotrimeric form of the pre-hairpin intermediate of gp41, MMM, is considered to be fusion-active. If the calculations are repeated assuming that the heterotrimer, MML, containing only one molecule of $N36^{Mut(e,g)}$, is also fusion-active, the resulting theoretical curves do not reproduce the experimental data. One can therefore conclude that the energetics of formation of a five-helix bundle comprising a heterotrimeric internal coiled-coil consisting of two N-helices of gp41 and one $N36^{Mut(e,g)}$ helix surrounded by two C-helices of gp41 is not sufficiently favorable to bring the target and viral membranes into sufficiently close proximity for fusion to take place.

Concluding Remarks—Using rational design, we have engineered two peptides derived from the N-helix of the ectodomain of gp41. The parent peptide, N36, corresponds to residues 546–581 of HIV-1 Env and encompasses the N-terminal helix of gp41. The $N36^{Mut(a,d)}$ peptide was designed to remove interactions leading to self-association and the formation of a trimeric coiled-coil of N-helices while preserving those residues that interact with the C-helix of the ectodomain of gp41. The absence of any fusion-inhibitory activity of $N36^{Mut(a,d)}$ leads us to conclude that the C-region of gp41 can only interact with a trimeric coiled-coil of N-helices. The $N36^{Mut(e,g)}$ peptide was designed to preserve the interactions leading to self-association while replacing those residues that interact with the C-region. $N36^{Mut(e,g)}$ forms a monodisperse trimer in solution that does not interact with the C-region of gp41 and yet still inhibits fusion about 50-fold more effectively than the native gp41 sequence (*i.e.* N36) from which it was derived. These results can only be explained by the existence of a dynamic equilibrium between monomeric and trimeric coiled-coil forms of the N-region of gp41 in the pre-hairpin intermediate on a time scale sufficiently fast to permit subunit exchange and the consequent formation of heterotrimers of the N-helices of gp41 and $N36^{Mut(e,g)}$. Thus, $N36^{Mut(e,g)}$ disrupts the homotrimeric coiled-coil of N-helices in the pre-hairpin intermediate state of gp41 and represents a novel third class of gp41-targeted fusion inhibitor. The other two classes of inhibitors bind to either the homotrimeric coiled-coil of N-helices (*e.g.* C34 and T20) or to the exposed C-region (*e.g.* N_{CCG}-gp41 and 5-helix) of gp41 in the pre-hairpin intermediate state. Since C34 (and presumably T20) also binds to N_{CCG}-gp41 and 5-helix (19, 20), these two classes of inhibitors antagonize each other. In contrast, one would predict that the $N36^{Mut(e,g)}$ class of inhibitors should act either additively or synergistically with either of the other two classes. Therefore, $N36^{Mut(e,g)}$ may represent a promising lead for the design of clinically effective, novel fusion inhibitors.

Acknowledgments—We thank A. Szabo for stimulating discussions, I. Nesheiwat and L.C. Chang for technical assistance, E. Berger for soluble CD4, and L. Pannell for mass spectrometry.

REFERENCES

1. Freed, E. O., and Martin, M. A. (1995) *J. Biol. Chem.* **270,** 23883–23886
2. Eckert, D. M., and Kim, P. S. (2001) *Annu. Rev. Biochem.* **70,** 777–810
3. Moore, J. P., Trkola, A., and Dragic, T. (1997) *Curr. Opin. Immunol.* **9,** 551–562
4. Caffrey, M., Cai, M., Kaufman, J., Stahl, S. J., Wingfield, P. T., Covell, D. G., Gronenborn, A. M., and Clore, G. M. (1998) *EMBO J.* **17,** 4572–4584
5. Chan, D. C., Fass, D., Berger, J. M., and Kim, P. S. (1997) *Cell* **89,** 263–273
6. Weissenhorn, W., Dessen, A., Harrison, S. C., Skehel, J. J., and Wiley, D. C.

(1997) *Nature* **387,** 426–430
7. Tan, K. J., Liu, J., Wang, S., Shen, S., and Lu, M. (1997) *Proc. Natl. Acad. Sci. U. S. A.* **94,** 12303–12308
8. Malashkevich, V. N., Chan, D. C., Chutkowski, C. T., and Kim, P. S. (1998) *Proc. Natl. Acad. Sci. U. S. A.* **95,** 9134–9139
9. Wild, C. T., Oas, T., McDanal, C. B., Bolognesi, D., and Matthews, T. J. (1992) *Proc. Natl. Acad. Sci. U. S. A.* **89,** 10537–10541
10. Wild, C. T., Shugars, D. C., Greenwell, T. K., McDanal, C. B., and Matthews, T. J. (1994) *Proc. Natl. Acad. Sci. U. S. A.* **91,** 9770–9774
11. Chan, D. C., Chutkowski, C. T., and Kim, P. S. (1998) *Proc. Natl. Acad. Sci. U. S. A.* **95,** 15613–15617
12. Eckert, D. M., and Kim, P. S. (2001) *Proc. Natl. Acad. Sci. U. S. A.* **98,** 11187–11192
13. Furuta, R. A., Wild, C. T., Weng, Y., and Weiss, C. D. (1998) *Nat. Struct. Biol.* **5,** 276–279
14. Chan, D. C., and Kim, P. S. (1998) *Cell* **93,** 681–684
15. Kilby, J. M., Hopkins, S., Venetta, T. M., DiMassimo, B., Cloud, G. A., Lee, J. Y., Alldredge, L., Hunter, E., Lambert, D., Bolognesi, D., Matthews, T., Johnson, M. R., Nowak, M. A., Shaw, G. M., and Saag, M. S. (1998) *Nat. Med.* **4,** 1302–1307
16. Pozniak, A. (2001) *J. HIV Res.* **6,** 92–94
17. Weissenhorn, W., Dessen, A., Calder, L. J., Harrison, S. C., Skehel, J. J., and Wiley, D. C. (199) *Mol. Membr. Biol.* **16,** 3–9
18. Kliger, Y., and Shai, Y. (2000) *J. Mol. Biol.* **295,** 163–168
19. Louis, J. M., Bewley, C. A., and Clore, G. M. (2001) *J. Biol. Chem.* **276,** 29485–29489
20. Root, M. J., Kay, M. S., and Kim, P. S. (2001) *Science* **291,** 884–888
21. Wingfield, P. T., Stahl, S. J., Kaufman, J., Zlotnick, A., Hyde, C. C., Gronenborn, A. M., and Clore, G. M. (1997) *Protein Sci.* **6,** 1653–1660
22. Caffrey, M., Kaufman, J., Stahl, S. J., Wingfield, P. T., Gronenborn, A. M., and Clore, G. M. (1999) *Protein Sci.* **8,** 1904–1907
23. Peisajovich, S. G., and Shai, Y. (2001) *J. Mol. Biol.* **311,** 249–254
24. Bohm, G., Muhr, R., and Jaenicke, R. (1992) *Protein Eng.* **5,** 191–195
25. Perkins, S. J. (1986) *Eur. J. Biochem.* **157,** 169–180
26. Salzwedel, K., Smith, E., Dey, B., and Berger, E. J. (2000) *J. Virol.* **74,** 326–333
27. Chance, E. M., Curtis, A. R., Jones, I. P., and Kirby, C. R. (1979) *FACSIMILE, Atomic Energy Research Establishment Report R8775*, Harwell, H. M. Stationary Office, London, UK
28. Clore, G. M. (1983) in *Computing in Biological Science* (Geisow, M. J., and Barrett, A. N., eds) pp. 313–348, Elsevier/North-Holland, New York
29. Lu, M., Blacklow, S. C., and Kim, P. S. (1995) *Nat. Struct. Biol.* **2,** 1075–1082
30. Jones, P. L., Korte, T., and Blumenthal, R. (1998) *J. Biol. Chem.* **273,** 404–409
31. Muñoz-Barroso, I., Durell, S., Sakaguchi, K., Appella, E., and Blumenthal, R. (1998) *J. Cell Biol.* **140,** 315–323